

LINEARISED MODELLING OF TURBULENT DRAG-REDUCTION USING STREAMWISE-TRAVELLING WAVES OF WALL-NORMAL VELOCITY

H. Ahmad ,Fuaad P.A, M.F. Baig & M.S. Naim
Department of Mechanical Engineering
Aligarh Muslim University, Aligarh-202002
mfbaig.me@amu.ac.in

ABSTRACT

Numerical experiments have been performed for modelling turbulent drag-reduction due to active-control of streamwise-travelling wall-normal waves using a linearised Navier-Stokes model in a turbulent channel flow. The effect of control on the transient growth of near-wall turbulent streaks and production of turbulent kinetic energy is studied. Simulations for a wide range of phase speeds have been performed at a fixed wave-amplitude and percentage amplification/reduction in the streak strength has been computed. The streak amplification from linearised-simulations has been compared with the percent-change in turbulent wall shear-stress from DNS data and a power-law relationship has been observed between the two.

1 Introduction

A sizable number studies for achieving skin-friction drag reduction in the turbulent flows have shown that implementation of open loop active-control in form of streamwise travelling waves of wall-normal velocity (*STWNV*) show inhibitory effect on near-wall turbulence. Among the initial studies, Aamo *et al.* (2003) employed a pressure-based feedback control to explore the effectiveness of wall-transpiration to produce turbulent-drag reduction. Their results for 2-D transient flow-fields showed instantaneous drag far lower than in corresponding laminar flow. DNS study by Min *et al.* (2006) showed skin-friction drag in a turbulent channel can be sustained below that in corresponding laminar flow by employing a blowing and suction induced upstream travelling waves and the key mechanism that produced this sub-laminar drag was generation of positive near-wall Reynolds shear stress by the control.

Majority of control-studies in turbulence-research are DNS studies, consequently the researchers have been restricted to study low or moderate Reynolds number turbulent shear flows. Moreover, they have also been constrained from studying the effects of every realizable combination of κ (streamwise wavenumber), ω (oscillation frequency) and W_0 (amplitude) of these travelling waves on the turbulent drag. This led researchers to use the linearised models to investigate the effect of control on turbulent drag. The argument behind linearised modelling of the near-wall turbulence stems from the works of Landahl (1989), who

proposed that evolution of near-wall streaks is governed by a linear mechanism where the nonlinear terms serve as localised disturbance sources. Important contributions in understanding the generation mechanism of near-wall turbulence came from the works of Chernyshenko & Baig (2005). They showed that the near-wall turbulent streaks are formed by the combined action of wall-normal motion, mean-shear and diffusion which is implicit in the linearised Navier-Stokes equations (*LNSE*). The *LNS* equations alongwith properly selected nonlinear source terms provide a numerically efficient way to study the generation and growth process of near-wall streaks. Exploiting these advantages of *LNSE*, Duque-Daza *et al.* (2012) modelled turbulent skin-friction drag by performing linearised-simulations to analyse the impact of travelling waves of spanwise wall-velocity in turbulent boundary layers. They computed the percentage amplification of turbulent kinetic energy of the streaks for a wide range of phase-speeds and compared their results to the DNS results of Quadrio *et al.* (2009). A close correlation observed between the two gave a strong implication that a linear mechanism was fundamental in bringing about turbulent skin-friction reduction/augmentation.

This paper intends to investigate the effects of *STWNV* having a fixed wave-amplitude on the transient-growth of near-wall streaks in a turbulent channel flow at a fixed $Re_\tau = 180$ over a broad parametric-range of κ and ω . Further, we aim to compare the results of *LNSE* for mitigating/augmenting streak-strength (in form of streamwise turbulent kinetic energy) in a controlled flow with the wall-shear stress computed using DNS study and to assess the level of agreement between the two.

2 Mathematical-formulation and Numerical-scheme

2.1 The governing equations and numerical algorithm

The form of *LNS* equations employed in this study are adopted from Chernyshenko & Baig (2005), in which the basic flow state (represented by U_i, P) was statistically split into a linear combination of mean flow (represented by \bar{U}_i, \bar{P}) and a fluctuating flow (represented by u_i, p). These equations are non-dimensionalised for a turbulent channel flow choosing friction velocity (u_τ) as velocity-scale, half-channel height (δ) as length-scale, δ/u_τ as time-scale and

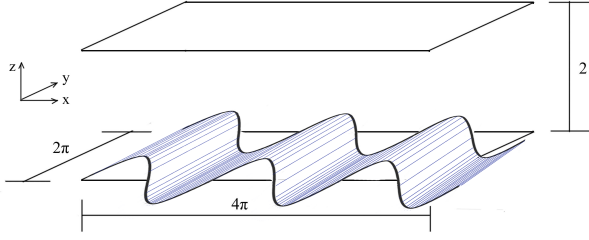


Figure 1. Schematic of the plane channel with streamwise-travelling wall-normal waves.

ρu_τ^2 as the pressure-scale. The *LNS* equations are expressed in tensorial form as:

$$\frac{\partial u_i}{\partial x_i} = 0 \quad (1)$$

$$\frac{\partial u_i}{\partial t} + \bar{U}_j \frac{\partial u_i}{\partial x_j} + u_j \frac{\partial \bar{U}_i}{\partial x_j} = -\frac{\partial p}{\partial x_i} + \frac{1}{Re_\tau} \left(\frac{\partial^2 u_i}{\partial x_j \partial x_j} \right) + \tilde{f}_i \quad (2)$$

where \tilde{f} represents an artificial body-force term which actually represents the effects of nonlinear terms of the N-S equations and is mathematically written as:

$$\tilde{f}_i = -\frac{\partial \bar{U}_i}{\partial t} - u_j \frac{\partial u_i}{\partial x_j} - \bar{U}_j \frac{\partial \bar{U}_i}{\partial x_j} - \frac{\partial \bar{P}}{\partial x_i} - \frac{1}{Re_\tau} \left(\frac{\partial^2 \bar{U}_i}{\partial x_j \partial x_j} \right) \quad (3)$$

It generates highly energetic cross-flow perturbations which interact with the mean-flow profile through the linear coupling term *i.e.* $w \frac{\partial \bar{U}}{\partial z}$ and this eventually leads to the formation of near-wall streaks (Kim & Lim (2000); Schmid & Henningson (2001)). The transient growth of these near-wall streaks is dictated by eqns. (1) and (2). Figure 1 shows the schematic representation of the physical domain for a fully turbulent flow through a planar channel for a fixed friction Reynolds number $Re_\tau = 180$, having a wall-normal height of 2δ , while the streamwise and spanwise periodic domains are $4\pi\delta$ and $2\pi\delta$, respectively, where δ was numerically equal to 1. The choice of computational domain for the simulations performed has been so chosen so that the disturbances decay to 5% of their maximum value when they reach the streamwise end of the domain. A constant turbulent-mean velocity profile (for $Re_\tau = 180$) is imposed in streamwise direction to model a constant streamwise mean-pressure gradient required to drive the flow. The *LNS* equations are subject to no-slip on the solid walls (*i.e.* $u_i = 0$), translational periodicity for velocity and pressure in the spanwise direction and non-reflective boundary conditions at the exit (*i.e.* $\frac{\partial^2 u_j}{\partial x_i^2} = 0, \frac{\partial p}{\partial x_i} = 0$). At inflow, the perturbations are assumed to be absent *i.e.* $u_i = 0$, as they are generated by a source-term at a fixed location inside the domain. The disturbance pressure at the inflow and the walls is obtained from the momentum equation as $\frac{\partial p}{\partial x_i} = -\bar{U}_j \frac{\partial u_i}{\partial x_j} - u_j \frac{\partial \bar{U}_i}{\partial x_j} + \frac{1}{Re_\tau} \left(\frac{\partial^2 u_i}{\partial x_j^2} \right)$. The numerical scheme used is a two-step predictor-corrector algorithm, based on a modified version of Simplified Marker and Cell (*SMAC*) technique proposed by Cheng & Armfield (1995). A semi-implicit time integration methodology has been

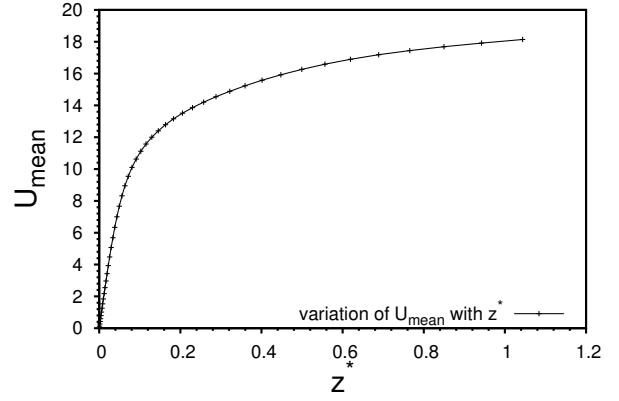


Figure 2. Turbulent mean velocity profile of plane Poiseuille turbulent flow at $Re_\tau = 180$.

used for treating the viscous terms implicitly which ensures stable solutions. Pressure-velocity decoupling is avoided by using momentum interpolation proposed by Rhie & Chow (1983). The correction Pressure-Poisson equation is solved using S.S.O.R preconditioned GMRES solver. The collocated mesh employed had uniform spacing in streamwise and spanwise directions, taken as $\Delta x^+ = 17.40$ & $\Delta y^+ = 17.14$, respectively. While in wall-normal direction, the spacing of the first grid-point with respect to the wall is $\Delta z^+ = 0.18$ and there are 5 grid points in $z^+ < 1$ and 20 points in $z^+ < 10$ region. The mesh employs 131 points each in streamwise and wall-normal direction and 67 grid-points in spanwise direction, respectively.

2.2 Selection of the initial conditions & quantification of the transient growth.

The base-flow is a classical mean-profile $\bar{U}(z)$ for a plane turbulent channel flow at $Re_\tau = 180$ and it combines a Musker profile from the wall to the overlap region and a Coles wake function for the outer part till half-height of the channel (Nagib & Chauhan (2008)). The kind of velocity profile employed in *LNS*-solver is shown in Figure 2. For modelling the nonlinear source-term, Low-Order Model (*LOM*) approach proposed by Lockerby *et al.* (2005) is used. *LOM* deals with implementation of a body-force in form of a concentrated vorticity source placed in the buffer layer and it is mathematically represented by a double delta function $\delta(x - x_f)\delta(z - z_f)$ in streamwise and wall-normal directions. The forcing term used in current study emulates a localised Gaussian vorticity source such that the different components of nonlinear body force field are given by $\tilde{f}_x = 0, \tilde{f}_y = 0, \tilde{f}_z = Gz^2 e^{-a(x-x_f)^2 - b(z-z_f)^2}$. Here G is the magnitude of forcing, a and b are parameters defining the width of the Gaussian function while x_f and z_f denote the location of the forcing in x and z directions, respectively. In the current study these parameters are chosen based on numerical-experiments as $G = 1.0, a = 110.0, b = 500.0, x_f = 1.014, z_f = 0.025$ in order to excite length scales which yield 18 pairs of high and low-speed streaks that decay to 5% of the maximum u as they reach the outflow boundary.

The temporal variation of streak strength was recorded using a measure based on streamwise turbulent kinetic-energy *STKE* (E_v) (eqn. 4) of these streaks at three different wall-normal planes in the viscous-sublayer and buffer-layer

regions, *i.e.* at $z^+ = 5, 10$ and 20 , respectively in a similar way as proposed by Chernyshenko & Baig (2005).

$$E_v(x, y, a, t) = \int_0^{L_x} \int_0^{L_y} u^2(t)|_{z^+=a} dx dy \quad (4)$$

Here L_x, L_y denote the maximum domain length of the channel in x, y directions, respectively while $z^+ = a$ denotes the particular wall-normal plane at which measure is computed. This methodology computes spatio-temporal measure of *STKE*, as any inhibitive/augmentative effect of control on the transient growth of near-wall streaks leads to weaker/stronger magnitudes of *STKE* which are directly proportional to reduction/enhancement of turbulent skin-friction drag.

3 Implementation of STWNV-control in the linearised-solver

The basic flow state is a mean turbulent-channel velocity profile $\bar{U}(z)$ alongwith impulsively generated turbulent-perturbations while the active-control is in the form of purely two-dimensional streamwise-travelling wall-normal waves that are generated at the bottom-wall of the channel by a continuous suction and blowing (of zero net mass-flux) which is mathematically represented in form of a travelling cosine-wave as $\bar{W}_{wall} = W_0 \cos(\kappa x - \omega t)$. As argued by Woodcock *et al.* (2011), the resulting flow in the channel could be seen as a combination of three mathematical variables *i.e.* a mean turbulent flow in streamwise direction $\bar{U}(z)$, a 3-D perturbation field (u, v, w and p) and a convection-induced flow in the near-wall region due to wall suction and blowing ($\bar{W}(x, z, t)$) which is predominantly 2-D in nature. Hence, the governing equation for control is the following equation for mean-flow in z -direction is:

$$\begin{aligned} \frac{\partial \bar{W}}{\partial t} + \bar{U} \frac{\partial \bar{W}}{\partial x} + \bar{V} \frac{\partial \bar{W}}{\partial y} + \bar{W} \frac{\partial \bar{W}}{\partial z} = \\ - \frac{\partial \bar{P}}{\partial z} + \frac{1}{Re_\tau} (\nabla^2 \bar{W}) - \frac{\partial \bar{w}u}{\partial x} - \frac{\partial \bar{w}v}{\partial y} - \frac{\partial \bar{w}w}{\partial z} \end{aligned} \quad (5)$$

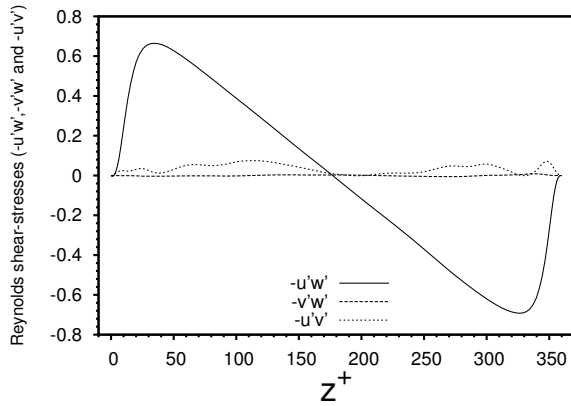
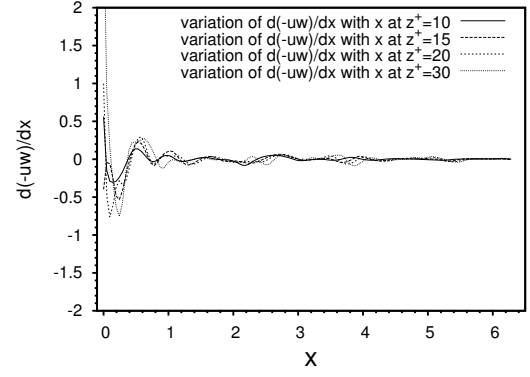
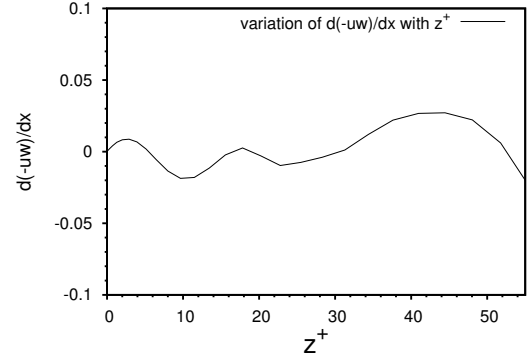


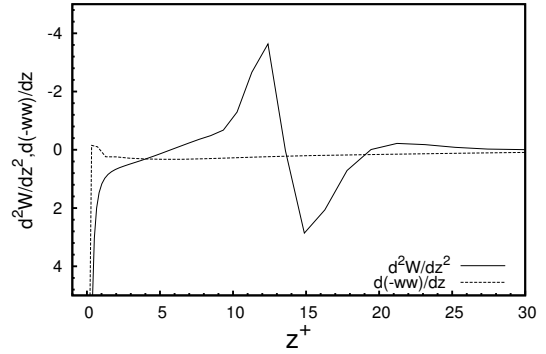
Figure 3. Comparison of the order of magnitudes of different Reynolds shear stresses in a turbulent flow with STWNV-control



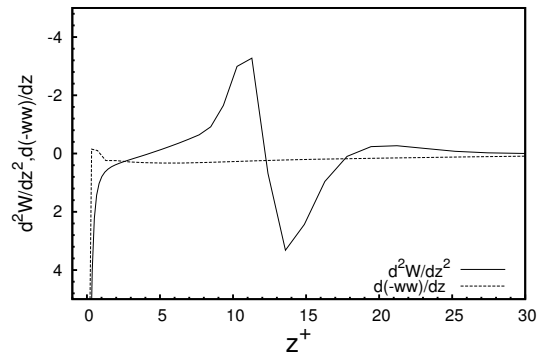
(a)



(b)



(c)



(d)

Figure 4. Comparison of $\frac{\partial^2 \bar{W}}{\partial z^2}$ (a) with streamwise gradient of Reynolds shear stresses $-\frac{\partial \bar{u}w}{\partial x}$ at different wall normal planes, (b) in wall-normal direction with $-\frac{\partial \bar{u}w}{\partial x}$ computed locally at a streamwise location and with wall-normal gradient of $-\frac{\partial \bar{w}w}{\partial z}$ in the near-wall region at two different times (c) $t^+ = 72$, (d) $t^+ = 144$, respectively in a turbulent flow with STWNV-control.

As the control is purely 2-D, there is no dependence of mean flow properties on y-coordinate which means $\bar{V} = 0$. Min *et al.* (2006) argued that the linear analysis assumes turbulent mean-profile to be unaffected by the perturbations generated by the wall suction and blowing. The amplitude W_0 of the travelling wave was selected as 0.35 (1.9% of centreline-velocity) to exploit the results of stability-analysis by Lee *et al.* (2008) who showed that mean-flow profile $\bar{U}(z)$ remains unchanged on applying *STWNV*-control with wave-amplitudes around 1.5% of centreline-velocity. Moreover, the results of DNS study conducted by Ahmad *et al.* (2015) show that the mean-flow profile remains symmetric and unchanged in the near-wall region $z^+ \leq 20$ on the application of *STWNV*. This implies that the control mainly affects the Reynolds shear stresses $-\overline{u'w'}$ while the viscous stresses remain unchanged in comparison to the uncontrolled flow. DNS also shows that the mean-flow profile $\bar{U}(z)$ is invariant in time as well as in stream-wise and spanwise directions, respectively in space. Further, DNS computations by Ahmad *et al.* (2015) showed that for $W_0 = 0.35$, $\frac{\partial \bar{P}}{\partial z}$ was negligibly smaller than $\frac{\partial \bar{P}}{\partial x}$ (≈ 1.0). Further it showed that $-\overline{uv}$, $-\overline{vw}$ were negligible in comparison to $-\overline{uw}$ (refer Figure. 3). Collective analysis of instantaneous variation of gradient of viscous stresses $\frac{\partial^2 \bar{W}}{\partial z^2}$ showed them to be at least 40 times larger than $\frac{\partial \overline{uw}}{\partial x}$. Figure. 4(a) shows the streamwise variation of $\frac{\partial \overline{uw}}{\partial x}$ along different wall normal planes at which the significant magnitudes of viscous stresses exist while Fig. 4(b) shows the variation of $\frac{\partial \overline{uw}}{\partial x}$ in wall-normal direction computed locally for a streamwise location. Also the gradient of Reynolds stress $\frac{\partial \overline{uw}}{\partial z}$ were found to be negligible in comparison to the gradient of viscous-stresses at two different time instants (as is evident from Figs. 4(c) & 4(d), respectively) and hence the effect of these Reynolds-stress gradients (*i.e.* $\frac{\partial \overline{uw}}{\partial x}$ and $\frac{\partial \overline{uw}}{\partial z}$) were neglected based on similar arguments of Quadrio & Ricco (2011). Hence, the governing-equation for the control finally modifies to the form:

$$\frac{\partial \bar{W}}{\partial t} + \bar{U} \frac{\partial \bar{W}}{\partial x} + \bar{W} \frac{\partial \bar{W}}{\partial z} = \frac{1}{Re_\tau} \left(\frac{\partial^2 \bar{W}}{\partial x^2} + \frac{\partial^2 \bar{W}}{\partial z^2} \right) \quad (6)$$

which is solved simultaneously with *LNSE* at every time-step in order to supply the active-control to the flow. It is apparent from eqn. (6) that there is a one way coupling of \bar{U} affecting \bar{W} accompanied with the wall-normal advection of \bar{W} by itself. At the bottom-wall, the same cosine wave-equation serves as boundary condition alongwith no-slip for \bar{U} , while the top-wall is subjected to no-slip for all the velocity components.

4 Results and Discussions

Linearised simulations were performed on the uncontrolled turbulent channel flow as well as on the flow with active-control of *STWNV* for different values of streamwise wavenumber (κ^+) and oscillation-frequency (ω^+) in order to explore a wide range of $\kappa^+ - \omega^+$ parametric space. Here κ^+ ranges from 0 to 0.028 while ω^+ ranges from -0.28 to 0.28. A total of 145 simulations were performed by varying $\Delta \kappa^+$ in steps of 0.0056 and $\Delta \omega^+$ in steps of 0.011. The temporal-measure of streamwise turbulent kinetic energy *STKE* (E_v) was integrated in time as $\mu = \int (E_v) dt$ and

then percent-amplification (ε) of streak-strength was computed using the expression proposed by Duque-Daza *et al.* (2012):

$$\varepsilon_{z^+=a} = \frac{\mu_{uncontrolled} - \mu_{controlled}}{\mu_{uncontrolled}} \times 100\% \quad (7)$$

For each case, the time-integration for μ was performed until the magnitude of streamwise perturbation velocity decrease to 5% of the maximum value (*i.e.* $u \approx 5\%$ of u_{max}), except for three cases of drag-increase where the time-integration for μ was performed till $u \approx 20 - 30\%$ of u_{max} . These three cases of drag-increase occur due to a strong non-linear phenomenon in the near-wall region on application of control. Figure 5(a) shows the comparison of time-history of streamwise *TKE* at $z^+ = 10$ for four different cases of downstream travelling waves with the uncontrolled case. It is seen that there is an increase as well as decrease in E_v for different cases of downstream travelling waves in comparison to the uncontrolled flow which implies that the downstream travelling waves leads to mitigation of turbulent perturbations for certain phase-speeds and also enhance the perturbations for other phase-speeds in the near-wall region. Figure 5(b) shows the comparison of measure E_v at $z^+ = 10$ for four different cases of upstream travelling waves with the uncontrolled case and we see that there is a reduction in the streamwise *TKE* implying that application of upstream travelling waves mostly leads to mitigation of turbulent-perturbations.

Figure 6 shows the contour plot obtained for percentage amplification/reduction of streamwise *TKE* ε of the near-wall streaks at wall-normal plane $z^+ = 10$, for a broad range of κ^+ and ω^+ . The positive values of ε show that $\mu_{controlled}$ is smaller than $\mu_{uncontrolled}$ indicating a reduction in streamwise *TKE* due to generation of weaker streaks by the action of *STWNV*-control while the converse holds good for negative values of ε . Positive values of ε signify reduction in turbulent skin-friction drag as *TKE* is directly proportional to drag at the wall(s) as argued by Duque-Daza *et al.* (2012). From the contour plot, we observe that reduction of ε (*i.e.* skin-friction drag-reduction) occurs in the entire region of parametric space except for a nearly-continuous inclined corridor where negative values of ε are observed indicating zones of increased skin-friction drag on application of control. This diagonal corridor of amplified disturbance-field starts from the region where slow upstream travelling waves are located and then spans through the region of downstream travelling waves with low streamwise wavenumbers (κ^+) before gradually fading away with increasing κ^+ . This observation is in consonance with the results of linear-analysis carried out by Min *et al.* (2006) who reported the presence of a narrow region in the parametric space, for downstream travelling waves and for slow upstream travelling waves, in which there was a significant increase in magnitudes of turbulent-drag which gradually reduced with increasing κ^+ . Moreover, the linearised-results of the contour plot for ε are in agreement with the DNS results of Ahmad *et al.* (2015) which also point towards the existence of a corridor of increased skin-friction drag for downstream travelling wall-normal waves having low and moderate values of κ^+ .

To show the effectiveness of *LNS*-simulations for investigation of skin-friction drag-reduction in a turbulent flow with *STWNV*-control, we need to trace relationship be-

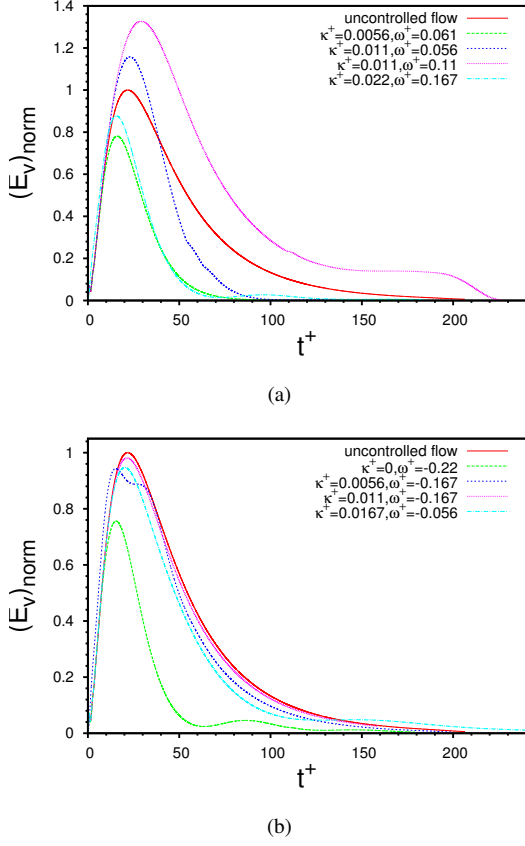


Figure 5. Comparison of the measure of streamwise TKE on application of (a) downstream travelling waves and (b) upstream travelling waves respectively, with the uncontrolled case at wall-normal plane $z^+ = 10$. Plots have been normalised by maximum streamwise TKE attained by the uncontrolled flow.

tween the results of linearised-simulations and DNS study. Hence, from the DNS study of Ahmad *et al.* (2015), instantaneous percent-change in turbulent skin friction ($\Delta\tau\%$) was computed using the instantaneous wall shear-stress (τ_{wall}) as:

$$\Delta\tau\% = \frac{\tau_{wall}^c - \tau_{wall}^{uc}}{\tau_{wall}^{uc}} \times 100\% \quad (8)$$

where τ_{wall}^{uc} stands for wall-shear stress in uncontrolled-flow while τ_{wall}^c stands for wall-shear stress in controlled flow. The percent-change in turbulent skin-friction $\Delta\tau\%$ obtained at the bottom-wall of the channel is compared with the percent-amplification in streak-strength (ϵ) computed at wall-normal plane $z^+ = 10$ and a striking similarity between the numerical prediction of drag-reduction/augmentation by two methodologies is observed, as listed in Table ?? . This shows that due to the action of control, when there is a reduction of the shear-stress at the controlled wall, there is a simultaneous reduction of $STKE$ in the near-wall region and these two quantities are directly proportional to each other. Moreover, there is a strong implication that a linear mechanism plays a fundamental role in inhibiting/enhancing turbulent drag reduction via streamwise-travelling waves of wall normal velocity. In order to correlate between the results of LNS and DNS methodologies, instantaneous percent-change in turbulent skin friction

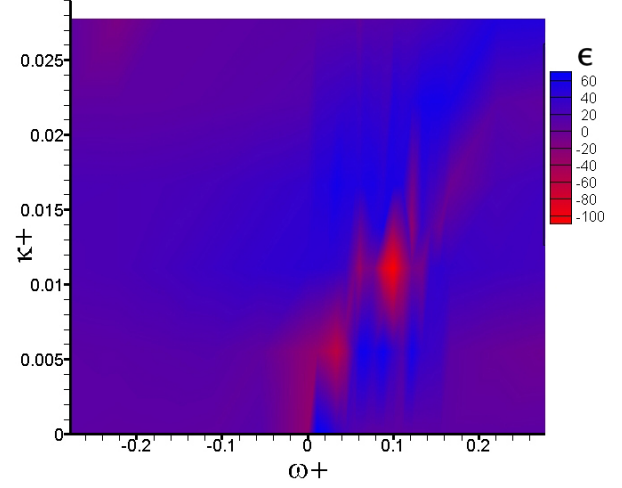


Figure 6. Contour plot for percent-change in amplification of streamwise TKE (ϵ) of streaks at $z^+ = 10$ over the parametric space (κ^+ , ω^+)

$\Delta\tau\%$ is plotted against streak-amplification factor ϵ for the wall-normal plane $z^+ = 10$ in the buffer-layer region. For this discrete data-set, a relationship is obtained which is mathematically expressed as:

$$\Delta\tau\% = 5.3217(\epsilon^{0.2323}) \quad (9)$$

Table 1. Table showing comparison between % change in turbulent skin-friction drag $\Delta\tau\%$ from DNS and streak-amplification factor ϵ at $z^+ = 10$.

Case	κ^+	ω^+	c^+	$\Delta\tau\%$ obtained from DNS	ϵ at $z^+ = 10$ from linear analysis
S1	0	0.1667	∞	7.23446	7.83428
S2	0.0056	-0.1667	-30.0	10.18735	12.40697
S3	0.0111	-0.1667	-15.0	11.99291	25.22914
S4	0.1111	-0.1667	-1.5	9.02102	5.18676
S5	0.0556	0.00278	0.05	8.56092	11.96837

The relationship obtained between percent-change in turbulent skin friction ($\Delta\tau\%$) obtained at the controlled-wall and streak-amplification factor (ϵ) which is based on the measure of $STKE$ is governed by a power-law relationship as shown by eqn. 9.

5 Summary

We investigated the effect of active-control of streamwise travelling waves of wall-normal velocity with varying phase-speeds on the transient-growth of near-wall turbulent streaks using the LNS equations. The upstream travelling waves at almost all phase-speeds and downstream travelling waves of moderately low phase-speeds were found to be most efficacious in bringing about turbulent drag-reduction as reflected in the contour plot for percent change in amplification of streamwise TKE of streaks at $z^+ = 10$. For the downstream travelling waves, a reduction in TKE

for travelling waves of low and moderate phase speeds was observed in the contour-plot while the high phase speed waves made-up a narrow corridor of increased TKE in which enhanced turbulent skin-friction drag occurred. Comparison between $\Delta\tau\%$ and ε showed that there exists a direct-correlation between the skin-friction reduction/augmentation obtained from DNS studies and the percent-change in streak-amplification calculated from LNS simulations, thereby implying that the linear mechanism of streak growth plays a fundamental role in causing drag-reduction.

Acknowledgement

The authors gladly acknowledge useful discussions with Dr. Nadeem Hasan on this work.

REFERENCES

- Aamo, O. M., Krstic, K. & Bewley, T. R. 2003 Control of mixing by boundary feedback in two-dimensional channel flow. *Automatica* **39**, 1597–1606.
- Ahmad, H., Baig, M. F. & Fuaad, P. A. 2015 Numerical investigation of turbulent-drag reduction induced by active control of streamwise travelling waves of wall-normal velocity. *European Journal of Mechanics - B/Fluids* **49**, 250–263.
- Cheng, L. & Armfield, S. 1995 A simplified marker and cell method for unsteady flows on non-staggered grids. *International Journal for Numerical Methods in Fluids* **21**, 15–34.
- Chernyshenko, S. I. & Baig, M. F. 2005 The mechanism of streak formation in near-wall turbulence. *Journal of Fluid Mechanics* **544**, 99–131.
- Duque-Daza, C. A., Baig, M. F., Lockerby, D. A., Chernyshenko, S. I. & Davies, C. 2012 Modelling turbulent skin-friction control using linearized navierstokes equations. *Journal of Fluid Mechanics* **702**, 403–414.
- Kim, J. & Lim, J. 2000 A linear process in wall-bounded turbulent shear flows. *Physics of Fluids* **12**, 1885–1888.
- Landahl, M. T. 1989 Boundary layer turbulence regarded as a driven linear system. *Physica D* **37**, 11–19.
- Lee, C., Min, T. & Kim, J. 2008 Stability of a channel flow subject to wall blowing and suction in the form of a traveling wave. *Physics of Fluids* **19** (8), 101513.
- Lockerby, D. A., Carpenter, P. W. & Davies, C. 2005 Control of sublayer streaks using microjet actuators. *AIAA Journal* **43**, 1878–1886.
- Min, T., Kang, S.M., Speyer, L. J. & Kim, J. 2006 Sustained sub-laminar drag in a fully developed channel flow. *Journal of Fluid Mechanics* **558**, 309–318.
- Nagib, H.M. & Chauhan, K.A. 2008 Variations of von-karman coefficient in canonical flows. *Physics of Fluids* **20**, 101518.
- Quadrio, M. & Ricco, P. 2011 The laminar generalized stokes layer and turbulent drag-reduction. *Journal of Fluid Mechanics* **667**, 135–157.
- Quadrio, M., Ricco, P. & Viotti, C. 2009 Streamwise travelling waves of spanwise wall-velocity for turbulent drag-reduction. *Journal of Fluid Mechanics* **627**, 161–178.
- Rhie, C. M. & Chow, W. L. 1983 Numerical study of the turbulent flow past an airfoil with trailing edge separation. *AIAA Journal* **21**, 1525–1532.
- Schmid, P. J. & Henningson, D. S. 2001 *Stability and Transition in Shear Flows*. Springer.
- Woodcock, J. D., Sader, J. E. & Marusic, I. 2011 Induced flow due to blowing and suction flow control: an analysis of transpiration. *Journal of Fluid Mechanics* **690**, 366–398.